

# The impacts of dew-induced foliar shielding on the energy, water and isotope balance of leaves

Cynthia Gerlein-Safdi<sup>1</sup>, Craig James Sinkler<sup>2</sup>, Kelly Krispin Caylor<sup>1</sup>

<sup>1</sup> Princeton University, Department of Civil and Environmental Engineering,  
E-208 E-Quad, Princeton, NJ 08544, USA

<sup>2</sup> Rider University, 2083 Lawrenceville Road, Lawrenceville, NJ 08648, USA

Author for correspondence: *Cynthia Gerlein-Safdi*

Tel: +1-609-865-5428

Email: *cgerlein@princeton.edu*

<b>Total word count</b> (excluding summary, references and legends)	6443
Summary	198
Introduction	1219
Materials and Methods	2890
Results	476
Discussion	1801 (28% of total)
Acknowledgements	57
No. of Figures	7 (all color except No. 6)
No. of Tables	2
No. of Supporting Information files	2 figures (all color)

## Summary

- The uptake of water from the surface of the leaves, called foliar uptake, is common when rainfall is scarce and non-meteoric water (dew or fog) is the only water source. However, many species have very water repellent leaves. Past studies have not differentiated between the uptake of water and the impact of the droplets on the energy balance of the leaf, which we call ‘foliar shielding’.
- Leaves of the hydrophobic *Colocasia esculenta* were sprayed with isotopically enriched water. We developed a protocol using a laser spectrometer and an induction module for the rapid analysis of leaf samples. The leaf water potential and water isotopes were monitored for different water-stress conditions.
- Dew-treated leaves exhibited a higher leaf water potential ( $P < 0.05$ ) and c. 30% decrease in transpiration rate ( $P < 0.001$ ) compared to the control. The dew treated leaves also had a depleted water isotopic composition compared to the control ( $P < 0.001$ ). Three possible mechanisms are proposed for the interaction of water droplets with the leaf energy and water balance.
- Comparing three previous foliar uptake studies to our results, we conclude that foliar shielding has a comparable yet opposite effect to foliar uptake on leaf water isotopes.

**Key words:** *Colocasia esculenta*, dew, foliar uptake, foliar shielding, induction module, laser spectrometer, leaf energy balance, leaf water isotopes

<sup>1</sup> I. Introduction

<sup>2</sup> Non-meteoric water is an important source of water for many plants, because it occurs consistently in all  
<sup>3</sup> environments. But since it only provides small amounts of water, it is often overlooked in large scale  
<sup>4</sup> models greater than the ecosystem level. Plants from many different environments have long been known  
<sup>5</sup> to be using fog [Stanton and Horn, 2013, Eller et al., 2013, Berry and Smith, 2014] or dew [Andrade, 2003,  
<sup>6</sup> Clus et al., 2008, Lakatos et al., 2012, Berkelhammer et al., 2013] through foliar uptake. The literature sug-  
<sup>7</sup> gesting the importance of this mechanism is growing and includes a wide range of plant species and areas.

<sup>8</sup> So far, most studies focused on determining circumstances in which specific plants use foliar uptake  
<sup>9</sup> as a source of water. Vegetation in dry and fog-prone areas like coastlands [Burgess and Dawson, 2004,  
<sup>10</sup> Stanton and Horn, 2013] or mountain hillsides [Berry et al., 2014a] have adapted to using fog as their main  
<sup>11</sup> source of water. Similarly, dew water has been shown to be a major source of water on islands where fresh  
<sup>12</sup> water is scarce [Clus et al., 2008] or by species that have physical features allowing them to collect dew water,  
<sup>13</sup> like epiphytic bromeliads [Andrade, 2003] or lichens [Lakatos et al., 2012]. Both of these plants grow on  
<sup>14</sup> other plants, often without any access to soil water.

<sup>15</sup> In the present study, we will focus on the interaction of non-meteoric water droplets on the leaf en-  
<sup>16</sup> ergy balance, which we call ‘foliar shielding’. It is known that many species have water-repellent leaves  
<sup>17</sup> [Neinhuis and Barthlott, 1997] which are not adapted to uptake water. For most plants, non-meteoric water  
<sup>18</sup> deposition is a source of nuisance as it may freeze and cause damages to the leaf in cold climate, or stag-  
<sup>19</sup> nate and cause rotting and pathogen infection in warm environments [Evans et al., 1992]. Leaves that are  
<sup>20</sup> repeatedly exposed to dew have even been shown to become more water-repellent [Aryal and Neuner, 2009].  
<sup>21</sup> However, micro-droplets of water will indeed form on the surface of even very hydrophobic leaves. The  
<sup>22</sup> interaction of these droplets on the leaf energy balance (foliar shielding) has been mentioned in previous  
<sup>23</sup> work [Limm et al., 2009, Berkelhammer et al., 2013], but this study is the first to quantify the impact of this  
<sup>24</sup> process on leaf water balance and leaf water isotopes.

<sup>25</sup> **Leaf energy balance —** Because they are unable to move to the shade, leaves are vulnerable to sun  
<sup>26</sup> radiation, and they can often be warmer than the surrounding air. The leaf temperature will in turn affect the  
<sup>27</sup> saturation vapor pressure, isotope fractionation, transpiration, and photosynthesis. Smaller leaves tend to  
<sup>28</sup> be at a temperature closer to the ambient air, since their boundary layer is thinner. This is the reason why,  
<sup>29</sup> on a single tree, leaves exposed to the sun are usually smaller than shaded ones. To stay cool, leaves use a  
<sup>30</sup> combination of re-radiation (transfer of energy to the surroundings), convection (heat loss as cool air moves  
<sup>31</sup> over the surface of the leaf) and evaporative cooling (evaporation of water inside the leaf into water vapor,  
<sup>32</sup> which is an exothermic process) [Vogel, 2012]. During a drought, leaves have to preserve water to maintain

33 turgor pressure, which competes with evaporative cooling. In this case, leaves are left with re-radiation and  
34 convection to cool themselves down. This is sometimes not enough to maintain a low temperature. If its  
35 duration extends for too long, a drought might lead to plant mortality.

36 Non-meteoric water can supply the plants with a pool of water that will supplement the scarce leaf  
37 water by depositing a layer of small water droplets on the surface of the leaves. This provides a form of  
38 externalized evaporative cooling. Moreover, the presence of the droplets will both increase the albedo of  
39 the leaves, allowing it to reflect more energy [Pinter, 1986], and increase surface roughness, which increases  
40 the leaf boundary layer, therefore decreasing the vapor pressure deficit (VPD) and lowering the evaporative  
41 demand. This later mechanism was proposed by [Limm et al., 2009] to explain how fog suppresses nighttime  
42 respiration in redwoods.

43 Foliar shielding is therefore directly affecting the water status of the leaf by influencing the leaf  
44 energy cycle. Depending on temperature and relative humidity, dew deposition can take from c. 1.5  
45 [Abtew and Melesse, 2012] to 6 hours [Monteith, 1957] after sunrise to completely evaporate from the sur-  
46 face of the leaves. Dew and fog can also form in the late afternoon before sunset [Wilson et al., 1999,  
47 Kabela et al., 2009]. Although neither dew nor fog is usually present at the hottest hour of the day, they can  
48 effectively shorten the duration of the water-stressed part of the day. This may significantly help the plant  
49 maintain its water status over an extended period of drought [Madeira et al., 2002, Proctor, 2012].

50 Dew formation is usually included in global climate models (GCMs) as it merely involves tracking dry  
51 bulb temperatures going below the dewpoint temperature. However, its interaction with vegetation is not  
52 commonly taken into account. Non-meteoric water deposition events occur around the world, even in dryland  
53 ecosystems [Agam and Berliner, 2006], and may affect large areas at the same time. The small changes in  
54 the energy, water and carbon balance of each single leaf can therefore have a large cumulative impact at  
55 the ecosystem level. Including this interaction into GCMs would allow modelers to better understand the  
56 response of vegetation to climate change and the feedback on CO<sub>2</sub> atmospheric concentrations.

57 **Leaf water isotopes** Foliar shielding will influence leaf water isotopes by decreasing leaf transpiration  
58 and leaf water enrichment in heavy isotopes [Farquhar et al., 2006, Cernusak and Kahmen, 2013]. The  
59 balance of the stable isotopologues of water has been used for decades to understand plant water fluxes  
60 [Allison et al., 1985, Ehleringer and Dawson, 1992, Werner et al., 2012], but as the number of water sources  
61 and sinks increases, the interpretation of isotope data can become difficult. The effect of foliar shielding  
62 on leaf water isotopes is, for example, likely to be opposite to that of foliar uptake of heavy fog or dew  
63 [Scholl et al., 2010], which will enrich leaf water in heavy isotopes. However, foliar uptake studies have so  
64 far not taken foliar shielding into account, even though it likely results in an underestimation of the amount of  
65 water uptaken by the leaf.

66 In this study, we present three experiments that focus on the effects of water droplets deposition at the  
67 surface of *Colocasia esculenta* leaves. This species is native to South East Asian tropical forests but has  
68 been cultivated across the world for many centuries under the name of taro. With a contact angle of  $\sim 164^\circ$   
69 [Neinhuis and Barthlott, 1997], *Colocasia esculenta* is considered to have highly water-repellent leaves. Its  
70 leaves can reach a size of up to c. 50 cm in length and c. 40 cm in width. We present the first protocol for the  
71 fast analysis of small sized leaf samples, allowing for spatial and temporal high-resolution mapping of the  
72 leaf-water properties. Using isotopically-labelled water as well as traditional plant physiology techniques, we  
73 confirm that the *Colocasia esculenta* leaves do not uptake water from the surface of the leaves. So far, few  
74 studies have attempted to map leaf isotopes because it is both time and labor intensive. While the number of  
75 replica presented in this study was limited by the novelty of the protocol, c. 550 plant samples were analyzed.  
76 This number largely exceeds the number of samples analyzed by previous studies focused on spatial patterns  
77 of leaf-water isotopes [Gan et al., 2002, Šantrůček et al., 2007]. We analyze the spatial patterns of leaf water  
78 isotopic enrichment and compare them to three different models. In addition, we show that foliar shielding  
79 decreases leaf transpiration and increases water potential, and we present three mechanisms that explain the  
80 influence of water droplet deposition on the energy and water cycles of water-repellent leaves. Finally, we  
81 compare our results to multiple foliar uptake studies. We conclude that foliar shielding has an opposite and  
82 larger effect on leaf isotopes than foliar uptake. It is therefore crucial to include foliar shielding in leaf isotope  
83 models to properly interpret isotope data of foliar uptake.

## 84 II. Materials and Methods

### 85 II.1 The added value of stable isotopes

86 Stable isotopes of water hold great potential for resolving transpiration and evaporation fluxes across multiple  
87 scales [Griffis et al., 2010, Rothfuss et al., 2012, Wang et al., 2013]. The process of evaporation is accompa-  
88 nied by a high degree of isotopic fractionation that leads to evaporated water with an isotopic composition  
89 depleted in the heavy isotopologues  $H_2^{18}O$  and  $HD^{16}O$ . This is due to the difference in vapor pressure of the  
90 different isotopologues [Farquhar et al., 2006]. Isotopic compositions are commonly expressed in terms of  
91 the relative ratios

$$\delta_i = \left( \frac{R_i}{R_{r_i}} - 1 \right) \times 10^3 \quad (1)$$

92 of isotope ratios [Mook, 2006], where  $\delta_i$  is expressed in ‰, and the index  $i$  stands for either  $^{18}O$  or D.  
93  $R_{^{18}O} = [H_2^{18}O]/[H_2^{16}O]$  and  $R_D = [HD^{16}O]/[H_2^{16}O]$  are the isotope ratios, while the  $R_{r_i}$  are the ratios of  
94 the corresponding reference standard. For water, the reference is the Vienna Standard Mean Ocean Water  
95 (VSMOW).

96 Because precipitation condenses under conditions of equilibrium fractionation,  $\delta^{18}\text{O}$  and  $\delta\text{D}$  in precip-  
97 itation evolve along a line with slope c. 8, the global meteoric water line (GMWL) [Voelker et al., 2014].  
98 However, kinetic isotope effects associated with differences in diffusivity among the different isotopologues of  
99 water can lead to deviations from the GMWL [Farquhar et al., 2006]. For example, since HD $^{16}\text{O}$  diffusivity  
100 is greater than that of H $_2^{18}\text{O}$ , the water of a leaf that has undergone heavy transpiration will be more depleted  
101 in D than in  $^{18}\text{O}$  (Fig. 1). Deuterium excess (d-excess) is a widely used measure of how evaporated a pool  
102 of water (ocean, lake, leaf) is and is defined as d-excess =  $\delta\text{D} - 8 \times \delta^{18}\text{O}$ . The average d-excess for precipi-  
103 tation is c. 10‰. Lower d-excess values generally indicate that the pool has undergone some evaporation  
104 [Brooks et al., 2014] (Fig. 1).

105 Stable isotopes are also very efficient to identify different water sources in plants [Ehleringer and Dawson, 1992].  
106 Indeed, simple mixing models allow one to separate the composition and the fluxes coming from differ-  
107 ent sources [Phillips and Gregg, 2001]. For this reason, stable isotopes are great natural labels that can  
108 be used to track pathways of water within plants without harming them; they have been the method of  
109 choice for many studies looking at foliar uptake [Breshears et al., 2008, Limm et al., 2009, Eller et al., 2013,  
110 Berry et al., 2014b]. Indeed, non-meteoric water is usually enriched in heavy isotopes [Scholl et al., 2010],  
111 making it easy to trace even after entering the leaf.

## 112 II.2 Experiment 1A: Effects of foliar shielding on leaf isotopes in natural conditions

113 Our first experiment examines leaf scale spatial and temporal patterns of water isotopes induced by the  
114 presence or the absence of dew under natural conditions. Six bulbs of *Colocasia esculenta* were planted in  
115 separate pots. All pots were placed outside and received full sun for four weeks. During this time, all plants  
116 were heavily watered with tap water ( $\delta^{18}\text{O} \approx -5.96\text{\textperthousand}$ ,  $\delta\text{D} \approx -37.63\text{\textperthousand}$ ) to allow plant growth. Once the six  
117 plants reached maturity, watering stopped and the plants were moved to a shaded area to remove any sun  
118 exposure differences between the plants.

119 Watering stopped two days before the beginning of the treatment. The upper-leaf surfaces in three of  
120 the six pots were misted with isotopically-enriched water ( $\delta^{18}\text{O} \approx 8.85\text{\textperthousand}$ ,  $\delta\text{D} \approx 737.64\text{\textperthousand}$ ) every two days  
121 using a spray bottle. Any extra water would run off the leaves, leaving them covered in submillimeter-size  
122 droplets, which is approximately the natural size for dew-deposition drops [Defraeye et al., 2013]. The  
123 misting simulated dew and was always performed around 08:00h.

124 The three control pots were not watered and did not receive any mist. To avoid contact between the misted  
125 water and the soil in the pots, the surfaces of all pots were covered in wrapping plastic. Six leaves were  
126 collected between the beginning of the control/dew treatments and the end of the experiments, three weeks  
127 later. The sampling and the analysis are described in Section II.5.

128 **II.3 Experiment 1B: Effects of foliar shielding on leaf isotopes under high water stress**

129 Our second experiment was designed to artificially increase the contrast between the control and misted  
130 treatments from Experiment 1A. The plants from this former experiment were moved into the laboratory and  
131 well watered for multiple weeks to offset any effects from the first experiment. Two leaves of similar size and  
132 of the same *Colocasia esculenta* plant were cut at the junction of the petiole and the rachis and left to dry c.  
133 80 cm under a blue light (Eiko 1960 EBW, 500 W, 10500 lumens, color temperature of 4800 K). The entire  
134 experiment lasted four hours. During that time, the treated leaf was misted with isotopically-labelled water  
135 ( $\delta^{18}\text{O} \simeq 8.85\text{‰}$ ,  $\delta\text{D} \simeq 737.64\text{‰}$ ) every half-hour. The control leaf was left to dry without any intervention.  
136 After four hours, samples were collected from both leaves as described in Section II.5.

137 **II.4 Experiment 2: Effects of foliar shielding on leaf water potential**

138 In this final experiment, we focused on the effect of water droplet deposition on leaf water potential under  
139 high water stressed conditions. One leaf was cut at the junction of the petiole and the rachis and left to dry.  
140 Three different water stress conditions were tested here: natural drying (control), high heat drying, and high  
141 heat and mist. In the high heat case, the leaf was placed 80 cm under a blue light (Eiko 1960 EBW, 500 W,  
142 10500 lumens, color temperature of 4800 K) and left to dry between 8 and up to 10 hours. In the high heat  
143 and mist case, the leaf was also misted with ultra pure water every hour using a spray bottle. Again, surplus  
144 water was allowed to runoff, leaving the leaf covered in submillimeter size water droplets. Leaf disks of  
145 1 inch diameter were collected every hour. The surface of each leaf disk was wetted with ultra pure water,  
146 immediately sanded with ultra-fine sandpaper (3M, 600 grit sandpaper), and the water potential analyzed on a  
147 WP4C (Decagon Devices Inc.).

148 **II.5 Isotope analysis**

149 For the water isotope analysis, each leaf was sampled in 12 to 25 different locations depending on the size of  
150 the leaf. All of the sampling points were located on the same half of the leaf and each point consisted of four  
151 holes (6 mm diameter) punched next to each other forming a square. Each hole was punched as quickly as  
152 possible to avoid evaporation, which would influence the isotopic composition of the neighboring holes. Each  
153 leaf disk was then secured in an aluminum foil and inserted in a sealed vial. The entire leaf was sampled in  
154 one go. The prepared vials were then stored in the fridge until being analyzed.

155 The leaf samples were analyzed using an Induction Module (IM) combined to a Cavity Ring Down  
156 Spectrometer (CRDS) L2103-i from Picarro Inc. (Sunnyvale, CA, USA). The IM was set on the ‘normal  
157 leaf’ setting: the leaf disks did not appear carbonized and, after being dried in the oven at 60°C for 48 hours,  
158 they showed no decline in weight, proving that this setting dried the leaf samples completely. The IM was

159 equipped with a micro-combustion module, which has been proven to efficiently reduce the interferences due  
160 to the presence of organics (Kate Dennis, private communication) in water samples extracted from plants  
161 [West et al., 2010]. On average, each half-leaf was sampled in c. 18 different locations, which corresponds to  
162 c. 73 punched holes.

163 The entire sampling and IM analysis process lasted from 1.5 to 2 days per half leaf depending on the size  
164 of the leaf, which limited the number of replicas we were able to conduct for this study. However, the number  
165 of leaf disks sampled per leaf far exceeded the c. 25 samples per half leaf collected by [Gan et al., 2002]. In a  
166 different study, [Šantrůček et al., 2007] sampled c. 50 disks per half leaf, but the study was carried out only  
167 in one replicate for each of the two treatments because of time and money constraints. The size of our study  
168 is therefore a significant improvement on previous efforts to map spatial patterns of leaf water isotopes. In  
169 addition, the sampling scheme allowed us to look at the temporal evolution of the spatial patterns, which to  
170 the best of our knowledge, had never been done before.

171 **IM-CRDS analysis sequence** The IM has only been available commercially for a few years and the number  
172 of published studies making use of it is still very limited [Berkelhammer et al., 2013]. Here we present the  
173 first detailed protocol for the analysis of leaf samples.

174 The IM-CRDS analysis sequence was adapted from a protocol developed in [van Geldern and Barth, 2012]  
175 for liquid water samples. Following their notation, Table 1 presents the sequence of standards and samples.  
176 Six empty vials were run at the beginning of each run. The average water vapor content,  $\delta^{18}\text{O}$ , and  $\delta\text{D}$  for  
177 the six vials were measured and introduced in a mixing model that allowed us to retrieve the true isotopic  
178 composition of the sample analyzed. Reference water samples were run using the filter paper provided with  
179 the instrument and the same piece of filter paper was reused for all the injections of a single reference water.  
180 We found that 3  $\mu\text{l}$  of reference water was necessary to reproduce the amount of water contained by one  
181 punch hole of *Colocasia esculenta*. The data was corrected for drift and memory effects, and it was also  
182 rescaled back to VSMOW.

183 **IRIS and IRMS analysis** Ten samples were sent to the Center for Stable Isotope Biogeochemistry at  
184 the University of California in Berkeley for IRMS analysis. For the IRMS method,  $\delta\text{D}$  was obtained by  
185 chromium combustion using an H/Device (Thermo Finnigan, Bremen). Microliters of water were injected  
186 in the H/Device and reduced to  $\text{H}_2$  gas. The ratio of D/H was then measured on a Thermo Delta Plus mass  
187 spectrometer. For the  $\delta^{18}\text{O}$  analysis, water from standards and samples were pipetted into glass vials and  
188 quickly sealed. The vials were then purged with 0.2%  $\text{CO}_2$  in Helium and allowed to equilibrate at room  
189 temperature for at least 48 hours. The  $^{18}\text{O}$  in the  $\text{CO}_2$  was then analyzed by continuous flow using a Thermo  
190 Gas Bench II interfaced to a Thermo Delta Plus XL mass spectrometer (Wenbo Yang, private communication).

191 In this H<sub>2</sub>O-CO<sub>2</sub> equilibration method, the dissolved components (organic and/or inorganic) do not affect  
192 the values of δ<sup>18</sup>O [West et al., 2010]. For the IRIS analysis, 1.8 μl of water was injected into a vaporizer  
193 and the vapor was pushed through a MCM with dry air. The concentrations of H<sub>2</sub><sup>16</sup>O, H<sub>2</sub><sup>18</sup>O and HD<sup>16</sup>O were  
194 measured on a laser spectrometer (L2103-i) from Picarro Inc. (Sunnyvale, CA, USA).

195 The ten samples analyzed both by IRMS and IRIS were used to calculate the offset between the two  
196 techniques. All the samples that had been run exclusively by IRIS or IM-CRDS (and had not been analyzed  
197 by IRMS) were then corrected for this offset. The IM-CRDS method has not been widely used yet and  
198 protocols and precision analyses are still absent from the scientific literature. To justify the results from the  
199 IM-CRDS, we compared the values obtained from the extracted water of the half-leaf analyzed by IRIS to the  
200 average leaf water composition obtained using a nearest neighbor interpolation on the half-leaf analyzed by  
201 IM-CRDS. For the seven leaves analyzed by IM-CRDS, the average difference between those two methods  
202 was 2.6±0.88‰ in δ<sup>18</sup>O (mean ± SE) and 3.4±2.4‰ in δD. One potential source of error comes from the  
203 IM-CRDS analyses being conducted on a different half of a leaf than the IRMS analyses. However, the average  
204 difference we observed between two halves of the same *Colocasia esculenta* leaf was 0.3±0.2‰ in δ<sup>18</sup>O and  
205 1.9±1.2‰ in δD. The differences between the results obtained with the IM-CRDS and the IRMS are therefore  
206 not attributable to the analyses being conducted on different halves of the same leaf. The number of studies  
207 making use of the fast analyzing capacity of the IM-CRDS is slowly growing [Berkelhammer et al., 2013],  
208 but further testing is still clearly necessary before using the IM-CRDS technique as an absolute method.  
209 However, our goal in this present study is to compare strongly enriched water samples and the order of the  
210 differences presented in the next section are up to two orders of magnitude greater than the error observed for  
211 the IM-CRDS. We therefore believe that the IM-CRDS is an appropriate method for our applications.

## 212 II.6 Linking d-excess and transpiration

213 While d-excess is commonly used in Atmospheric Science [Risi et al., 2013] and for interpreting ice core  
214 data [Luz et al., 2009], it has not been widely used in plant physiology. However, because it combines both  
215 deuterium and <sup>18</sup>O, d-excess contains more information than the isotopologues taken separately. Indeed,  
216 lower (more negative) d-excess values are associated with higher transpiration rates [Voelker et al., 2014]. To  
217 interpret d-excess differences in terms of transpiration rates, we link d-excess to steady-state relative humidity.  
218 The steady-state enrichment of leaf water Δ<sub>E</sub> above source water is expressed in [Farquhar et al., 2006] as

$$\Delta_E = (1 + \epsilon^*)[(1 + \epsilon_k)(1 - h) + h(1 + \Delta_v)] - 1 \quad (2)$$

219 where  $h$  is the relative humidity,  $\epsilon^*$  is the equilibrium fractionation;  $\epsilon^* = 9.2 \text{‰}$  ( $74 \text{‰}$ ) for  $\text{H}_2^{18}\text{O}$  (HDO) at  
220  $25^\circ\text{C}$  [Craig and Gordon, 1965]. The kinetic fractionation factor,  $\epsilon_k$ , is taken as

$$\epsilon_k^{\text{H}_2^{18}\text{O}} = \frac{28.5r_s + 18.9r_b}{r_b + r_s} \text{ and } \epsilon_k^{\text{HDO}} = \frac{16r_s + 10r_b}{r_b + r_s} \quad (3)$$

221 for  $\text{H}_2^{18}\text{O}$  and HDO, respectively [Farquhar et al., 1989, Farquhar et al., 2006].  $r_s$  is the stomatal resistance  
222 and it is taken to be constant and equal to  $217 \text{ s m}^{-2}$  [Hughes et al., 2014]. The resistance of the boundary  
223 layer,  $r_b$ , depends on leaf size and wind speed. Here we choose a constant leaf size of  $40 \text{ cm}$  and a wind  
224 speed of  $0.2 \text{ m s}^{-1}$ , resulting in an  $r_b = 1.13 \cdot 10^5 \text{ s m}^{-2}$ .  $\Delta_v$  is the enrichment of ambient water vapor above  
225 source water, which was calculated for a measured air composition of  $\delta^{18}\text{O} = -17 \text{‰}$  and  $\delta\text{D} = -100 \text{‰}$ .

226 The enrichment relative to a source can be linked back to isotopic compositions expressed in  $\delta$  notation  
227 through the relative ratios  $R$ :

$$\Delta_i = \frac{R_i}{R_{\text{source}}} - 1. \quad (4)$$

228 Using Equation 1 to express  $R_i$  as a function of  $\delta_i$ , we obtain a relation between  $\Delta_i$  and  $\delta_i$

$$\delta_i = \left[ \frac{(\Delta_i + 1) R_{\text{source}}}{R_{r_i}} - 1 \right] \times 1000. \quad (5)$$

229 By replacing  $\Delta_i$  in Equation 5 by its expression from Equation 2 and combining the expressions for  $\delta^{18}\text{O}$   
230 and  $\delta\text{D}$ , we obtain an expression for the d-excess as a function of the relative humidity  $h$ . We solve for  $h$ ,  
231 bounding its value between 0 and 1. Assuming that the vapor pressure inside the leaves,  $e_i$ , is at saturation,  
232 we may calculate the estimated transpiration rate  $E$  (in  $\text{mmol m}^{-2} \text{ s}^{-1}$ ) as

$$E = g_s \frac{e_i^* - h e_{\text{air}}^*}{P}. \quad (6)$$

233 Here,  $P$  is the atmospheric pressure taken to be  $101.3 \text{ kPa}$  and  $g_s$  (in  $\text{mmol m}^{-2} \text{ s}^{-1}$ ) is the stomatal conductance  
234 equal to  $1/r_s$ .  $e_i^*$  (in kPa) is the saturated vapor pressure calculated for a leaf temperature of  $25^\circ\text{C}$ .  $e_{\text{air}}^*$  (in  
235 kPa) is the saturated vapor pressure at air temperature, which is also taken to be  $25^\circ\text{C}$ . In our analysis, we  
236 compare the transpiration rates of dew treated leaves,  $E_{\text{dew}}$ , and that of control leaves,  $E_{\text{control}}$ .

## 237 II.7 Spatial patterns

238 Leaf water isotopic composition is often compared to the isotopic composition of freely evaporating water  
239 as described by the Craig-Gordon (CG) model [Craig and Gordon, 1965]. In this model, the fractionation is  
240 driven by the difference of saturation vapor pressure between the interior of the leaf and the atmosphere, and  
241 by the difference of diffusivity of the isotopologues. However, this simplistic model has been shown to largely

242 underestimate the actual isotopic enrichment. Two main models have since then been proposed to better  
 243 describe the complexity of leaf water isotopes patterns. The effect of the backward diffusion of enriched  
 244 water, a form of Péclet effect [Farquhar and Lloyd, 1993, Barbour et al., 2004], has been shown to improve  
 245 the prediction of bulk water enrichment, as well as the progressive enrichment of leaf water between the xylem  
 246 and the sites of evaporation [Gan et al., 2002]. The string-of-lakes effect takes into account the progressive  
 247 enrichment of leaf water along the path of water flow [Yakir et al., 1990, Helliker and Ehleringer, 2000] and  
 248 improves the modeling of large scale variations of leaf water enrichment.

249 The Craig-Gordon model of evaporation is expressed as [Gan et al., 2002]

$$\Delta_{CG} = \epsilon_k + \epsilon^* + (\Delta_v - \epsilon_k) \frac{h e_{air}^*}{e_i^*}, \quad (7)$$

250 with  $\Delta_v$  the isotopic enrichment of atmospheric water vapor relative to source water (Eq. 4).  $\epsilon_k$ ,  $r_b$ , and  $e_i^*$   
 251 depend on leaf temperature. Using an infrared picture of a *Colocasia esculenta* leaf, we are able to calculate  
 252  $\Delta_{CG}$  at each pixel to obtain a map of  $\Delta_{CG}$  that we compare to the spatial patterns of the measured isotopic  
 253 enrichment of leaf water relative to source water ( $\Delta_{lw}$ , as defined in Eq. 4). Based on meteorologic data  
 254 available for the duration of the experiment, pressure and relative humidity were taken to be constant and  
 255 equal to 1013 hPa and 80%, respectively.

## 256 II.8 Competing effects of foliar uptake and foliar shielding

257 To compare the relative effects of foliar uptake and foliar shielding, we analyze the results of three different  
 258 studies that conducted similar experiments on different species. [Limm et al., 2009] looked at a ten different  
 259 species from the coast redwood ecosystem of California (*Pseudotsuga menziesii* and *Sequoia sempervirens*  
 260 (conifers), *Polystichum munitum* and *Polystichum californicum* (ferns), *Oxalis oregana* (a short herbaceous),  
 261 *Arbutus menziesii*, *Gaultheria shallon*, *Vaccinium ovatum*, *Notholithocarpus densiflorus* and *Umbellularia*  
 262 *californica* (all evergreen broadleaf)), while [Eller et al., 2013] focused on *Drimys brasiliensis*, a woody  
 263 broadleaf evergreen native from Central and South America, and [Berry and Smith, 2014] concentrated on  
 264 *Abies fraseri* and *Picea rubens*, two montane conifers from the Appalachian Mountains. All the studies  
 265 conducted glasshouse experiments in which saplings experienced nighttime fog. Leaf samples were collected  
 266 in the evening before the fogging treatment and in the morning, right after the treatment. Every study used  
 267 isotopically labeled fog with a different composition ( $\delta D_{fog} - \delta D_{soil} = 16\text{\textperthousand}$  in [Berry and Smith, 2014],  
 268  $78\text{\textperthousand}$  in [Limm et al., 2009] and  $712\text{\textperthousand}$  in [Eller et al., 2013]). To compare the different experiments, we  
 269 normalized the results to reflect the leaf water enrichment that would have been observed if the fog water had  
 270 been  $20\text{\textperthousand}$  heavier than soil water, since this is within the range of natural values [Scholl et al., 2010].

271 **II.9 Statistical analysis**

272 Responses for the different experiments were analyzed using a two-sample t-test (Welch's t-test) with a 5%  
273 significance level. This test has been recognized as a better alternative to the Student's t-test when dealing  
274 with groups of unequal sample size or variance [Ruxton, 2006]. In the following, we will report the p-value,  
275 P, the test statistics, t, and the degrees of freedom of the test,  $\nu$ . When comparing the results of the different  
276 treatments in Experiments 1A and 1B, we treated the multiple samples collected on each leaf as a single  
277 population. *stat* and *syst* refer to the statistical and the systematic errors, respectively.

278 **III. Results**

279 **III.1 Water isotopes**

280 The results of Experiments 1A are presented as maps of the analyzed half leaves (Fig. 2). The maps were  
281 obtained using an inverse distance interpolation and show the evolution of the d-excess of leaves from the  
282 control and misted treatments collected at 0, 12 (dew), 14 (control) and 21 (dew and control) days from  
283 the beginning of the experiment. All the maps of  $\delta D$  and  $\delta^{18}O$  (Supporting Information, Fig.s S1 and S2)  
284 show a progressive enrichment [Cernusak and Kahmen, 2013] of leaf water when moving away from the  
285 main stem towards the rims of the leaf. The average difference between the center and the rim of the leaf for  
286 the five leaves presented is  $\Delta^{18}O = 11.1 \pm 1.2 \text{ ‰}$  (mean  $\pm$  SE) and  $\Delta D = 23.9 \pm 3.3 \text{ ‰}$ . When comparing the  
287 composition of the bulk water at the end of the experiment, the dew-treated leaf exhibits a d-excess higher by c.  
288 63.0‰ than the control one (two-sample t-test:  $t = -9.4$ ,  $\nu = 29$ ,  $P < 0.001$ ). There is no statistical difference  
289 between the treated and control leaves collected on days 12/14 (difference in mean d-excess  $\approx 10.2 \text{ ‰}$ ,  
290 two-sample t-test:  $t = -1.6$ ,  $\nu = 35$ ,  $P = 0.11$ ).

291 Similar maps were produced for Experiment 1B (Fig. 3). In this case, the heat lamp artificially increased  
292 the transpiration rate in both the control and the misted leaves, leading to significantly enriched  $\delta^{18}O$  and  
293  $\delta D$  values and low d-excess values for both treatments. The d-excess in the control case is c. 173.0 ‰ more  
294 negative than for the dew treated leaves (two-sample t-test:  $t = 3.9$ ,  $\nu = 29$ ,  $P < 0.001$ ). This experiment was  
295 merely an extreme version of Experiment 1A, with the objective of accentuating the contrast between the  
296 two treatments. While the high heat treatment led to a strong drying of some areas of the leaf, in particular  
297 those far away from the central vein, the significant difference observed between the control and the misted  
298 treatments do confirm the results of Experiment 1A.

299 **III.2 Leaf water potential**

300 Experiment 2 looks at the temporal evolution of water potential in artificially drying leaves (Fig. 4). Strong  
301 differences in drying pattern are shown for the misted and drought leaves. In both the control and the high  
302 heat and mist cases, the leaf water potential experiences a slow decline, which is well approximated by a  
303 linear function. However, the high heat treated leaves experience a faster decline and are better approximated  
304 by a parabola. Table 2 presents the average decline from initial to final leaf water potential for the three  
305 different treatments. All the data is normalized for leaf size and drying time. The decline in water potential  
306 was c. 64% smaller in the misted leaves than in the leaves subjected to the same high heat treatment but that  
307 did not get sprayed (two-sample t-test:  $t = 2.37, \nu = 7, P < 0.05$ ). The decline observed for misted leaves is  
308 not statistically different to the one observed for naturally drying leaves (two-sample t-test:  $t = -1.46, \nu = 6,$   
309  $P = 0.19$ ).

310 **IV. Discussion**

311 **IV.1 Foliar shielding-induced decrease in transpiration**

312 Treated leaves in Experiments 1A and 1B are all less enriched in heavy isotopes than control ones, despite  
313 being sprayed with highly enriched water ( $\delta^{18}\text{O} \simeq 8.85\ \text{\textperthousand}$ ,  $\delta\text{D} \simeq 737.64\ \text{\textperthousand}$ ), which is consistent with a lack  
314 of foliar uptake. Foliar shielding is then the only phenomenon inducing differences in leaf water d-excess  
315 composition between treated and control leaves. We apply the model described in Section II.6 to interpret our  
316 results in terms of the transpiration rate,  $E$ .

317 The use of a constant stomatal conductance and leaf temperature are most likely the largest sources  
318 of systematic error in this model. To calculate the systematic error associated with our choices for those  
319 parameters, we calculate  $E_{\text{dew}}/E_{\text{control}}$  for a range of leaf temperatures from  $10^\circ$  to  $40^\circ\text{C}$  and for a stomatal  
320 conductance  $g_s$  from 0.1 to 0.8  $\text{mmol m}^{-2} \text{s}^{-1}$ . We find that the systematic error associated with our choice of  
321  $g_s$  is negligible, while that associated with the choice of  $T_{\text{leaf}}$  is important for Experiment 1A, but not for  
322 Experiment 1B.

323 For Experiment 1A, the transpiration rate obtained for the dew treated leaf is significantly lower than that  
324 of the control ( $t = -9.4, \mu = 38, P < 0.0001$ ) by  $29.9 \pm 2.6$  (stat)  $\pm 1.1$  (syst) %. Similar results were found for  
325 Experiment 1B, where the dew treatment significantly ( $t = -3.9, \mu = 29, P < 0.0001$ ) decreased transpiration  
326 by  $29.9 \pm 9.1$  (stat) %. These values are consistent with [Garratt and Segal, 1988], who estimated that the  
327 reduction in transpiration due to dewfall could reduce daily plant water use by c. 10%. This value was  
328 obtained for wheat plants associated with a low transpiration rate. Since *Colocasia esculenta* leaves are larger  
329 and have a higher transpiration rate, we expect the reduction to be larger in our case (see Section IV.2).

330 **Spatial patterns** To understand the spatial patterns observed in Fig. 2 and 3, we calculate the expected CG  
331 enrichment for  $^{18}\text{O}$  as described in Section II.7. We compare the results to the leaf water enrichment above  
332 source water,  $\Delta_{lw}$  measured for three leaves from Experiment 1A (Fig. 5). All three leaves tested show an  
333 enrichment on both side of the 1:1 line, which corresponds to the CG enrichment.

334 Leaf water depleted from the expected CG model points toward a larger importance of the Péclet  
335 effect, while samples located across the 1:1 line show a larger importance of the string-of-lakes effect  
336 [Gan et al., 2002]. *Colocasia esculenta* leaves seem to generally behave like a string-of-lakes, in which  
337 the enriched water leftover after transpiration increases the expected enrichment of the next pool. This  
338 effect has been shown to be particularly important in monocots, since they tend to have parallel veins with  
339 stomata located in-between them that act as enrichment sites [Helliker and Ehleringer, 2000]. Since *Colocasia*  
340 *esculenta* is a monocot itself, our result confirms the main importance of the string-of-lakes effect in monocots  
341 and expands previous work that has so far been concentrating on dicots [Yakir et al., 1990, Gan et al., 2002,  
342 Šantrůček et al., 2007] and only a few monocots [Helliker and Ehleringer, 2000, Gan et al., 2003]. We find  
343 a strong linear correlation ( $R^2 = 0.84$ ,  $P < 0.001$ ) between  $\Delta_{lw}/\Delta_{CG}$  and distance from the petiole (Fig. 6).  
344  $\Delta_{lw}/\Delta_{CG}$  appears to be smaller than 1 for samples close to the petiole, and larger than 1 at the tip of the leaf  
345 and at the rims. This pattern has already be observed in cotton leaves [Gan et al., 2002] and was pointed out  
346 as another characteristic trait of the string-of lakes effect.

347 **Temporal patterns** Leaves collected from both treatments on day 12 or 14 present results that disagree  
348 with the trends formed by the results of day 0 and 21 (Fig. 2). It is important to note that the plants were  
349 kept outside throughout the experiment and were therefore subjected to the daily variations of temperature  
350 and relative humidity, which both influence the transpiration rate as well as the isotopic composition. The  
351 dew-treated leaf collected on day 12 was sampled after a prolonged period of dry and hot weather that  
352 might have enhanced the transpiration despite the artificial dew treatment. This may explain why this leaf  
353 presents lower d-excess values than expected. A series of small rain events happened on the day preceding the  
354 collection of the first control leaf on day 14, which may have decreased the transpiration rate and increased  
355 the d-excess composition of the leaf.

## 356 IV.2 Leaf energy cycle

357 Our results show that the deposition of submillimeter size droplets allow the leaf to decrease its transpiration  
358 rate and maintain its water potential. The water balance of the leaf is influenced by the change in energy  
359 balance associated with the water droplets deposited at the surface through three distinct processes.

360 First, the deposited droplets increase the albedo of the leaf, allowing more of the radiation to be reflected  
361 away from the leaf. Depending on the direction of the incoming solar radiation, water can have an albedo as

362 high as 1 (perfect reflector) whereas typical values for leaves are c. 0.2 for visible light. The increase of vegetation  
363 albedo due to dew deposition has been observed in the field many times [Pinter, 1986, Zhang et al., 2012].  
364 By reflecting more radiation when they are wet, leaves will decrease the incoming shortwave radiation and  
365 consequently keep their temperatures lower. This will in turn reduce the evaporative demand and the leaf  
366 transpiration.

367 Second, the energy that is not reflected will be dissipated through the evaporation of the droplets. The  
368 dissipated energy will not contribute to the leaf energy budget. Moreover, because evaporation is an exothermic  
369 process, the evaporation of the water droplets will result in a cooling of the leaf surface. This will again  
370 reduce the evaporative demand and the transpiration.

371 Finally, the evaporation of the droplets will cause the air close to the leaf to have a higher relative humidity  
372 than the surrounding air [Defraeye et al., 2013], creating a moist micro-climate around the leaf [Jones, 1992].  
373 This will decrease the difference between the interstitial and the air vapor pressures, and reduce the flux of  
374 water vapor out of the leaf, namely transpiration. By decreasing the outward flow of water vapor, more CO<sub>2</sub>  
375 will be able to enter the leaf, increasing interstitial CO<sub>2</sub> concentration, photosynthesis, and water use efficiency.  
376 The increase in surface roughness associated with the presence of the droplets at the surface of the leaf will  
377 also contribute to increasing the size of the boundary layer. Water potential values are correlated with leaf  
378 relative water content [Maxwell and Redmann, 1978] and with stomatal conductance [Lhomme et al., 1998];  
379 by maintaining a higher water potential, the leaf will be able to open its stomata wider. CO<sub>2</sub> assimilation is  
380 in turn linearly correlated to stomatal conductance [Lambers et al., 2008]. As a result, by affecting the leaf  
381 energy cycle, foliar shielding will allow the leaf to maintain its water status and increase CO<sub>2</sub> assimilation  
382 through multiple mechanisms.

#### 383 IV.3 Implications for foliar uptake studies

384 By decreasing evaporation, foliar shielding suppresses the isotopic enrichment associated with leaf water  
385 transpiration [Farquhar et al., 2006]. Therefore, leaves undergoing foliar shielding will have a bulk isotopic  
386 composition lower (more depleted) than leaves that do not experience it. The average  $\delta D$  enrichment between  
387 the first and last days of collection for Experiment 1A were  $-9.1 \pm 3.7 \text{ ‰}$  (mean  $\pm$  SE) for the control leaf and  
388  $-27.9 \pm 2.9 \text{ ‰}$  for the dew treated leaf. This corresponds to a  $-18.8 \pm 6.6 \text{ ‰}$  difference in enrichment between  
389 sprayed and control treatments. In the case of highly water stressed leaves (Experiment 1B, Fig. 3), the  
390 difference in enrichment reaches  $-45.2 \pm 35.8 \text{ ‰}$ .

391 Non-meteoric water is usually more enriched in deuterium than rain and soil water by up to 50 ‰  
392 [Scholl et al., 2010]. If foliar uptake is indeed happening in a leaf, the uptake of heavy fog water will then  
393 enrich the leaf water, while foliar shielding depletes leaf water in heavy isotopes. [Limm et al., 2009] pointed  
394 out the tension between foliar uptake and nighttime suppression of respiration due to the saturated atmosphere

395 during fog events. Transpiration is a much larger water loss for plants than respiration and the effects of foliar  
396 shielding during day time is expected to be have a even larger impact on leaf isotopes than that discussed by  
397 [Limm et al., 2009].

398 Using previous studies on foliar uptake (described in Section II.8), we were able to compare the relative  
399 impact of both processes. Foliar uptake has the largest impact on conifers (Fig. 7), where the difference in  
400 enrichment between treatment and control reaches up to c. 20 %. Foliar shielding for the non-water stressed  
401 case (Experiment 1A) exhibits the opposite effect, with a magnitude similar to the largest foliar uptake case.  
402 In the water stressed case (Experiment 1B), the depletion observed is as large as c. 45.2 %. The three foliar  
403 experiments presented here all used nighttime treatment, so foliar shielding did not impact the enrichment  
404 observed. However, the competing effects of foliar uptake and foliar shielding are likely to be very important  
405 when analyzing field or day time foliar uptake experiment data. For example, [Berry et al., 2014b] observed  
406 a significantly larger enrichment when fogging saplings in the morning than in the afternoon. This results is  
407 well explained if foliar shielding is taken into account, since foliar shielding will have a larger effect in the  
408 afternoon, when leaves are hotter and radiations stronger. Our results suggest that, in the field, foliar shielding  
409 might have a larger impact on leaf isotopes than foliar uptake.

410 The results of our study show a larger impact of foliar shielding in times of drought than in well-watered  
411 conditions. The simultaneous occurrence of non-meteoric water deposition and drought is common in  
412 drylands [Agam and Berliner, 2006], where many plants rely on non-meteoric water as their primary source  
413 of water [Stanton and Horn, 2013]. Regular dew formation has also been observed in the upper canopy of the  
414 Amazon forest during the dry season [Satake and Hanado, 2004, Frolking et al., 2011]. In those cases, the  
415 energy balance is thought to be the main driver of leaf water isotopic composition, with a response much  
416 larger than to soil water availability, for example [Wayland, 2015]. Foliar shielding will delay the time when  
417 leaves reach their maximum transpiration rate and attain isotopic steady state [Dubbert et al., 2014]. Isotopic  
418 steady state is often assumed when interpreting transpiration data, but [Dubbert et al., 2013] recently showed  
419 that this assumption is typically unjustified and can lead to errors in estimated transpiration fluxes by up to  
420 70%, since steady state models systematically overestimate the isotopic enrichment of leaf water. Isotopic  
421 steady state depends on the leaf transpiration rate, which changes quickly as energy flux incident on the leaf  
422 changes, for example when the leaf goes from the shade to the sun [Smith and Berry, 2013]. Foliar shielding  
423 has a large impact at short time scales on both leaf transpiration and water isotopes because of this fast  
424 response.

#### 425 **IV.4 Conclusion**

426 In this study, we used the highly hydrophobic leaves of *Colocasia esculenta* to look at the impacts of dew  
427 water droplets deposition (called foliar shielding) on the leaf energy, water and isotope balance. We show that

428 the spatial patterns of enrichment are consistent with the string-of-lakes model, which is common in monocots.  
429 Our results show that foliar shielding significantly decreases leaf transpiration by c. 30%, maintains leaf  
430 water potential, and limits leaf water isotopic enrichment. We highlight the opposite effects of foliar uptake,  
431 which enriches leaf water in heavy isotopes, and foliar shielding, which depletes it. Because both effects are  
432 of similar magnitude, taking both processes into accounts is crucial to properly interpret field data of foliar  
433 uptake.

434 **Acknowledgments**

435 The authors thank Todd Dawson and Wenbo Yang for the IRMS analysis, and Fulton Rockwell for the  
436 discussion on spatial patterns. C.Gerlein-Safdi and K.K. Caylor acknowledge the financial support of NASA  
437 Headquarters under the NASA Earth and Space Science Fellowship Program - Grant 14-EARTH14F-241 -  
438 and of the Science, Technology, and Environmental Policy Fellowship from the Princeton Environmental  
439 Institute.

## REFERENCES

- [Abtew and Melesse, 2012] Abtew, W. and Melesse, A. (2012). *Evaporation and Evapotranspiration - Measurements and Estimations*. Springer Science & Business Media.
- [Agam and Berliner, 2006] Agam, N. and Berliner, P. R. (2006). Dew formation and water vapor adsorption in semi-arid environments—A review. *Journal of Arid Environments*, 65(4):572–590.
- [Allison et al., 1985] Allison, G. B., Gat, J. R., and Leaney, F. W. J. (1985). The relationship between deuterium and oxygen-18 delta values in leaf water. *Chemical Geology: Isotope Geoscience section*, 58(1-2):145–156.
- [Andrade, 2003] Andrade, J. L. (2003). Dew deposition on epiphytic bromeliad leaves: an important event in a Mexican tropical dry deciduous forest. *Journal of Tropical Ecology*, 19(5):479–488.
- [Aryal and Neuner, 2009] Aryal, B. and Neuner, G. (2009). Leaf wettability decreases along an extreme altitudinal gradient. *Oecologia*, 162(1):1–9.
- [Barbour et al., 2004] Barbour, M. M., Roden, J. S., Farquhar, G. D., and Ehleringer, J. R. (2004). Expressing leaf water and cellulose oxygen isotope ratios as enrichment above source water reveals evidence of a Pécel effect. *Oecologia*, 138(3):426–435.
- [Berkelhammer et al., 2013] Berkelhammer, M., Hu, J., Bailey, A., Noone, D. C., Still, C. J., Barnard, H., Gochis, D., Hsiao, G. S., Rahn, T., and Turnipseed, A. (2013). The nocturnal water cycle in an open-canopy forest. *Journal of Geophysical Research: Atmospheres*, 118(1):10225.
- [Berry et al., 2014a] Berry, Z. C., Hughes, N. M., and Smith, W. K. (2014a). Cloud immersion: an important water source for spruce and fir saplings in the southern Appalachian Mountains. *Oecologia*, 174(2):319–326.
- [Berry and Smith, 2014] Berry, Z. C. and Smith, W. K. (2014). Experimental cloud immersion and foliar water uptake in saplings of *Abies fraseri* and *Picea rubens*. *Trees*, 28(1):115–123.
- [Berry et al., 2014b] Berry, Z. C., White, J. C., and Smith, W. K. (2014b). Foliar uptake, carbon fluxes and water status are affected by the timing of daily fog in saplings from a threatened cloud forest. *Tree Physiology*, 34(5):459–470.
- [Breshears et al., 2008] Breshears, D. D., McDowell, N. G., Goddard, K. L., Dayem, K. E., Martens, S. N., Meyer, C. W., and Brown, K. M. (2008). Foliar absorption of intercepted rainfall improves woody plant water status most during drought. *Ecology*, 89(1):41–47.

- [Brooks et al., 2014] Brooks, J. R., Gibson, J. J., Birks, S. J., Weber, M. H., Rodecap, K. D., and Stoddard, J. L. (2014). Stable isotope estimates of evaporation: inflow and water residence time for lakes across the United States as a tool for national lake water quality assessments. *Limnology and Oceanography*, 59(6):2150–2165.
- [Burgess and Dawson, 2004] Burgess, S. and Dawson, T. E. (2004). The contribution of fog to the water relations of *Sequoia sempervirens* (D. Don): foliar uptake and prevention of dehydration. *Plant, Cell & Environment*, 27(8):1023–1034.
- [Cernusak and Kahmen, 2013] Cernusak, L. A. and Kahmen, A. (2013). The multifaceted relationship between leaf water  $^{18}\text{O}$  enrichment and transpiration rate. *Plant, Cell & Environment*, 36(7):1239–1241.
- [Clus et al., 2008] Clus, O., Ortega, P., Muselli, M., Milimouk, I., and Beysens, D. (2008). Study of dew water collection in humid tropical islands. *Journal of Hydrology*, 361(1-2):159–171.
- [Craig and Gordon, 1965] Craig, H. and Gordon, L. I. (1965). Deuterium and oxygen-18 variations in the ocean and the marine atmosphere . *Proceedings of a Conference on Stable Isotopes in Oceanographic Studies and Palaeotemperatures*, pages 9–130.
- [Defraeye et al., 2013] Defraeye, T., Verboven, P., Derome, D., Carmeliet, J., and Nicolai, B. (2013). Stomatal transpiration and droplet evaporation on leaf surfaces by a microscale modelling approach. *International Journal of Heat and Mass Transfer*, 65:180–191.
- [Dubbert et al., 2013] Dubbert, M., Cuntz, M., Piayda, A., Maguás, C., and Werner, C. (2013). Partitioning evapotranspiration – Testing the Craig and Gordon model with field measurements of oxygen isotope ratios of evaporative fluxes . *Journal of Hydrology*, 496(C):142–153.
- [Dubbert et al., 2014] Dubbert, M., Cuntz, M., Piayda, A., and Werner, C. (2014). Oxygen isotope signatures of transpired water vapor: the role of isotopic non-steady-state transpiration under natural conditions. *New Phytologist*, 203(4):1242–1252.
- [Ehleringer and Dawson, 1992] Ehleringer, J. R. and Dawson, T. E. (1992). Water uptake by plants: perspectives from stable isotope composition. *Plant, Cell & Environment*, 15(9):1073–1082.
- [Eller et al., 2013] Eller, C. B., Lima, A. L., and Oliveira, R. S. (2013). Foliar uptake of fog water and transport belowground alleviates drought effects in the cloud forest tree species, *Drimys brasiliensis*(Winteraceae). *New Phytologist*, 199(1):151–162.

- [Evans et al., 1992] Evans, K. J., Nyquist, W. E., and Latin, R. X. (1992). A model based on temperature and leaf wetness duration for establishment of alternaria leaf-blight of muskmelon. *Phytopathology*, 82(8):890–895.
- [Farquhar et al., 1989] Farquhar, G., Hubick, K., Condon, A., and Richards, R. (1989). *Stable Isotopes in Ecological Research*, chapter Carbon isotope fractionation and plant water-use efficiency, pages 21–40. Springer New York.
- [Farquhar and Lloyd, 1993] Farquhar, G. and Lloyd, J. (1993). *Stable Isotopes and Plant Carbon-water Relations*, chapter Carbon and oxygen isotope effects in the exchange of carbon dioxide between terrestrial plants and the atmosphere, pages 47–70. Academic Press, New York.
- [Farquhar et al., 2006] Farquhar, G. D., Cernusak, L. A., and Barnes, B. (2006). Heavy water fractionation during transpiration. *Plant Physiology*, 143(1):11–18.
- [Frolking et al., 2011] Frolking, S., Milliman, T., Palace, M., Wisser, D., Lammers, R., and Fahnstock, M. (2011). Tropical forest backscatter anomaly evident in SeaWinds scatterometer morning overpass data during 2005 drought in Amazonia. *Remote Sensing of Environment*, 115(3):897–907.
- [Gan et al., 2003] Gan, K. S., Wong, S. C., and Yong, Jean Wan Hongand Farquhar, G. D. (2003). Evaluation of models of leaf water  $^{18}\text{O}$  enrichment using measurements of spatial patterns of vein xylem water, leaf water and dry matter in maize leaves. *Plant, Cell & Environment*, 26(9):1479–1495.
- [Gan et al., 2002] Gan, K. S., Wong, S. C., Yong, J. W. H., and Farquhar, G. D. (2002).  $^{18}\text{O}$  spatial patterns of vein xylem water, leaf water, and dry matter in cotton leaves. *Plant Physiology*, 130(2):1008–1021.
- [Garratt and Segal, 1988] Garratt, J. R. and Segal, M. (1988). On the contribution of atmospheric moisture to dew formation. *Boundary-Layer Meteorology*, 45(3):209–236.
- [Griffis et al., 2010] Griffis, T. J., Sargent, S. D., Lee, X., Baker, J. M., Greene, J., Erickson, M., Zhang, X., Billmark, K., Schultz, N., Xiao, W., and Hu, N. (2010). Determining the Oxygen Isotope Composition of Evapotranspiration Using Eddy Covariance. *Boundary-Layer Meteorology*, 137(2):307–326.
- [Helliker and Ehleringer, 2000] Helliker, B. R. and Ehleringer, J. R. (2000). Establishing a grassland signature in veins:  $^{18}\text{O}$  in the leaf water of C3 and C4 grasses. *PNAS*, 97(14):7894–7898.
- [Hughes et al., 2014] Hughes, N. M., Carpenter, K. L., Keidel, T. S., Miller, C. N., Waters, M. N., and Smith, W. K. (2014). Photosynthetic costs and benefits of abaxial versus adaxial anthocyanins in Colocasia esculenta ‘Mojito’. *Planta*, 240(5):971–981.

- [Jones, 1992] Jones, H. G. (1992). *Plants and microclimate: a quantitative approach to environmental plant physiology*. Cambridge University Press.
- [Kabela et al., 2009] Kabela, E. D., Hornbuckle, B. K., Cosh, M. H., Anderson, M. C., and Gleason, M. L. (2009). Dew frequency, duration, amount, and distribution in corn and soybean during SMEX05. *Agricultural and Forest Meteorology*, 149(1):11–24.
- [Lakatos et al., 2012] Lakatos, M., Obregón, A., Büdel, B., and Bendix, J. (2012). Midday dew - an overlooked factor enhancing photosynthetic activity of corticolous epiphytes in a wet tropical rain forest. *New Phytologist*, 194(1):245–253.
- [Lambers et al., 2008] Lambers, H., Chapin, III, F. S., and Pons, T. L. (2008). *Plant Physiological Ecology*. Springer Science & Business Media.
- [Lhomme et al., 1998] Lhomme, J. P., Elguero, E., Chehbouni, A., and Boulet, G. (1998). Stomatal control of transpiration: Examination of Monteith's formulation of canopy resistance. *Water Resources Research*, 34(9):2301–2308.
- [Limm et al., 2009] Limm, E. B., Simonin, K. A., Bothman, A. G., and Dawson, T. E. (2009). Foliar water uptake: a common water acquisition strategy for plants of the redwood forest. *Oecologia*, 161(3):449–459.
- [Luz et al., 2009] Luz, B., Barkan, E., Yam, R., and Shemesh, A. (2009). Fractionation of oxygen and hydrogen isotopes in evaporating water. *Geochimica et Cosmochimica Acta*, 73(22):6697–6703.
- [Madeira et al., 2002] Madeira, A. C., Kim, K. S., Taylor, S. E., and Gleason, M. L. (2002). A simple cloud-based energy balance model to estimate dew. *Agricultural and Forest Meteorology*, 111(1):55–63.
- [Maxwell and Redmann, 1978] Maxwell, J. O. and Redmann, R. E. (1978). Leaf water potential, component potentials and relative water content in a xeric grass, *Agropyron dasystachyum* (Hook.) Scribn. *Oecologia*, 35(3):277–284.
- [Monteith, 1957] Monteith, J. L. (1957). Dew. *Quarterly Journal of the Royal Meteorological Society*, 83:322–341.
- [Mook, 2006] Mook, W. G. (2006). *Introduction to Isotope Hydrology Stable and Radioactive Isotopes of Hydrogen, Carbon and Oxygen*. Taylor & Francis, London.
- [Neinhuis and Barthlott, 1997] Neinhuis, C. and Barthlott, W. (1997). Characterization and distribution of water-repellent, self-cleaning plant surfaces. *Annals of Botany*, 79(6):667–677.

- [Phillips and Gregg, 2001] Phillips, D. L. and Gregg, J. W. (2001). Uncertainty in source partitioning using stable isotopes. *Oecologia*, 127(2):171–179.
- [Pinter, 1986] Pinter, P. J. (1986). Effect of dew on canopy reflectance and temperature. *Remote Sensing of Environment*, 19(2).
- [Proctor, 2012] Proctor, M. C. F. (2012). Dew, where and when? 'There are more things in heaven and earth, Horatio, than are dreamt of in your philosophy...'. *New Phytologist*, 194(1):10–11.
- [Risi et al., 2013] Risi, C., Landais, A., Winkler, R., and Vimeux, F. (2013). Can we determine what controls the spatio-temporal distribution of d-excess and  $^{17}\text{O}$ -excess in precipitation using the LMDZ general circulation model? *Climate of the Past*, 9(5):2173–2193.
- [Rothfuss et al., 2012] Rothfuss, Y., Braud, I., Le Moine, N., Biron, P., Durand, J.-L., Vauclin, M., and Bariac, T. (2012). Factors controlling the isotopic partitioning between soil evaporation and plant transpiration: Assessment using a multi-objective calibration of SiSPAT-Isotope under controlled conditions. *Journal of Hydrology*, 442-443:75–88.
- [Ruxton, 2006] Ruxton, G. D. (2006). The unequal variance t-test is an underused alternative to Student's t-test and the Mann-Whitney U test. *Behavioral Ecology*, 17(4):688–690.
- [Šantrůček et al., 2007] Šantrůček, J., Kveton, J., Setlík, J., and Bulícková, L. (2007). Spatial variation of deuterium enrichment in bulk water of snowgum leaves. *Plant Physiology*, 143(1):88–97.
- [Satake and Hanado, 2004] Satake, M. and Hanado, H. (2004). Diurnal change of Amazon rain forest  $\sigma^0$  observed by Ku-band spaceborne radar. *IEEE Transactions on Geoscience and Remote Sensing*, 42(6):1127–1134.
- [Scholl et al., 2010] Scholl, M., Eugster, W., and Burkard, R. (2010). Understanding the role of fog in forest hydrology: stable isotopes as tools for determining input and partitioning of cloud water in montane forests. *Hydrological Processes*, 25(3):353–366.
- [Smith and Berry, 2013] Smith, W. K. and Berry, Z. C. (2013). Sunflecks? *Tree Physiology*, 33(3):233–237.
- [Stanton and Horn, 2013] Stanton, D. E. and Horn, H. S. (2013). Epiphytes as “filter-drinkers”: life-form changes across a fog gradient. *The Bryologist*, 116(1):34–42.
- [van Geldern and Barth, 2012] van Geldern, R. and Barth, J. A. C. (2012). Optimization of instrument setup and post-run corrections for oxygen and hydrogen stable isotope measurements of water by isotope ratio infrared spectroscopy (IRIS). *Limnology and Oceanography: Methods*, 10:1024–1036.

- [Voelker et al., 2014] Voelker, S. L., Brooks, J. R., Meinzer, F. C., Roden, J., Pazdur, A., Pawelczyk, S., Hartsough, P., Snyder, K., Plavcová, L., and Šantrůček, J. (2014). Reconstructing relative humidity from plant  $\delta^{18}\text{O}$  and  $\delta\text{D}$  as deuterium deviations from the global meteoric water line. *Ecological Applications*, 24(5):960–975.
- [Vogel, 2012] Vogel, S. (2012). *The Life of a Leaf*. The University of Chicago Press.
- [Wang et al., 2013] Wang, L., Niu, S., Good, S. P., Soderberg, K., McCabe, M. F., Sherry, R. A., Luo, Y., Zhou, X., Xia, J., and Caylor, K. K. (2013). The effect of warming on grassland evapotranspiration partitioning using laser-based isotope monitoring techniques. *Geochimica et Cosmochimica Acta*, 111:28–38.
- [Wayland, 2015] Wayland, H. (2015). An ecohydrological characterization of two African savanna trees under water stress. Master’s thesis, Princeton University.
- [Werner et al., 2012] Werner, C., Schnyder, H., Cuntz, M., Keitel, C., Zeeman, M. J., Dawson, T. E., Badeck, F. W., Brugnoli, E., Ghashghaei, J., Grams, T. E. E., Kayler, Z. E., Lakatos, M., Lee, X., Máguas, C., Ogée, J., Rascher, K. G., Siegwolf, R. T. W., Unger, S., Welker, J., Wingate, L., and Gessler, A. (2012). Progress and challenges in using stable isotopes to trace plant carbon and water relations across scales. *Biogeosciences*, 9(8):3083–3111.
- [West et al., 2010] West, A. G., Goldsmith, G. R., Brooks, P. D., and Dawson, T. E. (2010). Discrepancies between isotope ratio infrared spectroscopy and isotope ratio mass spectrometry for the stable isotope analysis of plant and soil waters. *Rapid Communications in Mass Spectrometry*, 24(14):1948–1954.
- [Wilson et al., 1999] Wilson, T. B., Bland, W. L., and Norman, J. M. (1999). Measurement and simulation of dew accumulation and drying in a potato canopy. *Agricultural and Forest Meteorology*, 93(2):111–119.
- [Yakir et al., 1990] Yakir, D., DeNIRO, M. J., and Gat, J. R. (1990). Natural deuterium and oxygen-18 enrichment in leaf water of cotton plants grown under wet and dry conditions: evidence for water compartmentation and its dynamics. *Plant, Cell & Environment*, 13(1):49–56.
- [Zhang et al., 2012] Zhang, Y.-f., Wang, X.-p., Pan, Y.-x., and Hu, R. (2012). Diurnal and seasonal variations of surface albedo in a spring wheat field of arid lands of Northwestern China. *International journal of Biometeorology*, 57(1):67–73.

## Figure Legends

**Figure 1:** Adapted from [Voelker et al., 2014]: Conceptual figure showing the evaporative conditions controlling the evolution of  $\delta^{18}\text{O}$  and  $\delta\text{D}$  in leaf water from source water located on the global meteoric water line (GMWL, dashed black line). The slope of the transpiration line depends on the relative humidity. The d-excess of a sample is the vertical distance from that sample to the d-excess reference line. The position of the source water along the GMWL depends on the temperature at which the water condensed and on the isotopic composition of the vapor.

**Figure 2:** Maps of the spacial distribution of d-excess of five *Colocasia esculenta* leaves collected throughout Experiment 1A. The maps were obtained by inverse distance interpolation of 12 to 25 sampling points analyzed on the Picarro Induction Module. All leaves are c. 38 cm long. **Left:** initial leaf collected on day 0. **Top row:** leaves collected on day 14 (center) and 21 (far right) from the control. **Bottom row:** leaves collected on day 12 (center) and 21 (far right) from the sprayed treatment, where the leaves were sprayed with isotopically enriched water ( $\delta^{18}\text{O} \approx 8.85\text{\textperthousand}$ ,  $\delta\text{D} \approx 737.64\text{\textperthousand}$ ) every two days. The color scheme is the same for all rows.

**Figure 3:** Maps of two leaves left to dry under a 500W blue light for four hours. **Top row:**  $\delta^{18}\text{O}$ ,  $\delta\text{D}$  and d-excess of the control (not sprayed) leaf. **Bottom row:**  $\delta^{18}\text{O}$ ,  $\delta\text{D}$  and d-excess of the leaf sprayed with isotopically enriched water ( $\delta^{18}\text{O} \approx 8.85\text{\textperthousand}$ ,  $\delta\text{D} \approx 737.64\text{\textperthousand}$ ) every half-hour. The control leaf shows higher enrichment and lower d-excess values that are associated with enhanced transpiration compared to the sprayed leaf.

**Figure 4:** Typical examples of the temporal evolution of the leaf water potential of *Colocasia esculenta* leaves under three different treatments. All the leaves under the natural drying (black circles) and the high heat and mist (blue diamonds) treatments are well fit by a linear relation (black dotted and blue dashed lines, respectively). All but one of the leaves under the high heat drying case (red squares) are better fit by a parabola (red solid line). All the leaves shown here are c. 38 cm long.

**Figure 5:** Comparison of the measured  $\Delta_{\text{lw}}$  and the Craig-Gordon predicted  $\Delta_{\text{CG}}$  for  $^{18}\text{O}$  in three leaves from Experiment 1A. **Black crosses:** initial leaf collected at day 0, **blue diamonds:** leaf collected on day 21 from the spray treatment, **red squares:** leaf collected on day 21 from the control. The black line represents a 1:1 relationship.

**Figure 6:** Ratio  $\Delta_{lw}/\Delta_{CG}$  for  $^{18}\text{O}$  in the leaf collected on day 21 from the control plant of Experiment 1A as a function of distance from the petiole relative to leaf total length ( $l_{max}$ ). The black line represents a linear fit.

**Figure 7:** A comparison between the impact of foliar uptake of nighttime fog in three studies [Limm et al., 2009, Eller et al., 2013, Berry and Smith, 2014] to foliar shielding in *Colocasia esculenta*. Bars represent the magnitude of the difference in enrichment between fogged/sprayed and control plants. Enrichment is the difference between pre- and post-treatment leaves. All the foliar uptake data were normalized to reflect enrichment corresponding to a realistic difference of 20 ‰ between rain and fog water [Scholl et al., 2010]. Error bars show one standard error. Because we did not obtain the raw data from the foliar experiments, error bars were not added for those, please refer to the original articles for more details.

## Supporting Information

Additional supporting information may be found in the online version of this article.

**Figure S1:** Interpolated maps showing the  $\delta D$  of the leaves analyzed in Experiment 1A.

**Figure S2:** Interpolated maps showing the  $\delta^{18}\text{O}$  of the leaves analyzed in Experiment 1A.

Identifiers		
ID	Type	Injections
Blank 1 to	Empty vial	1
Blank 6	Empty vial	1
DEST	Drift ref. water	10
HIS	High ref. water	10
ANTA	Low ref. water	10
DEST	Drift ref. water	10
HERA	QC ref. water	4
Sample 1 to	Sample	4
Sample 10	Sample	4
DEST	Drift ref. water	6
Sample 11 to	Sample	4
Sample 20	Sample	4
DEST	Drift ref. water	6

**Table 1:** Typical sequence layout of an IM-CRDS run with four reference waters. Following [van Geldern and Barth, 2012], HIS and ANTA are the names of the reference waters with high and low delta values, respectively. DEST and HERA are intermediate waters. DEST is the drift monitoring reference water, whereas HERA is treated as a sample for quality control. All reference waters except HERA are used for memory and VSMOW correction.

Treatment	Average drop in leaf water potential over 8h (MPa)	SE
Natural drying	0.43	0.03
High heat & mist	1.05	0.31
High heat	2.9	0.77

**Table 2:** Average drop in water potential (MPa) for the three treatments of Experiment 2: ‘Natural drying’ (control), ‘High heat and mist’ and ‘High heat’. Third column shows one standard error. All the data was normalized to reflect the drop in water potential for a 40 cm long leaf over 8 hours.

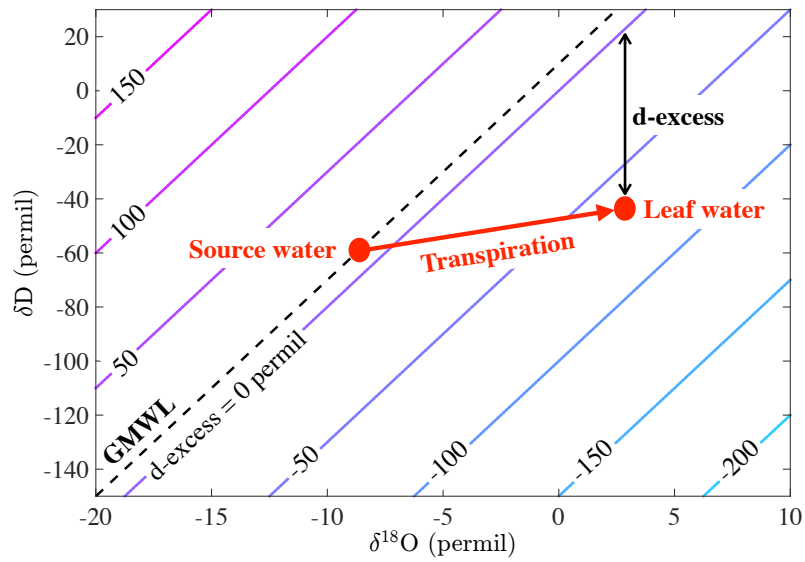


**Figure 1**

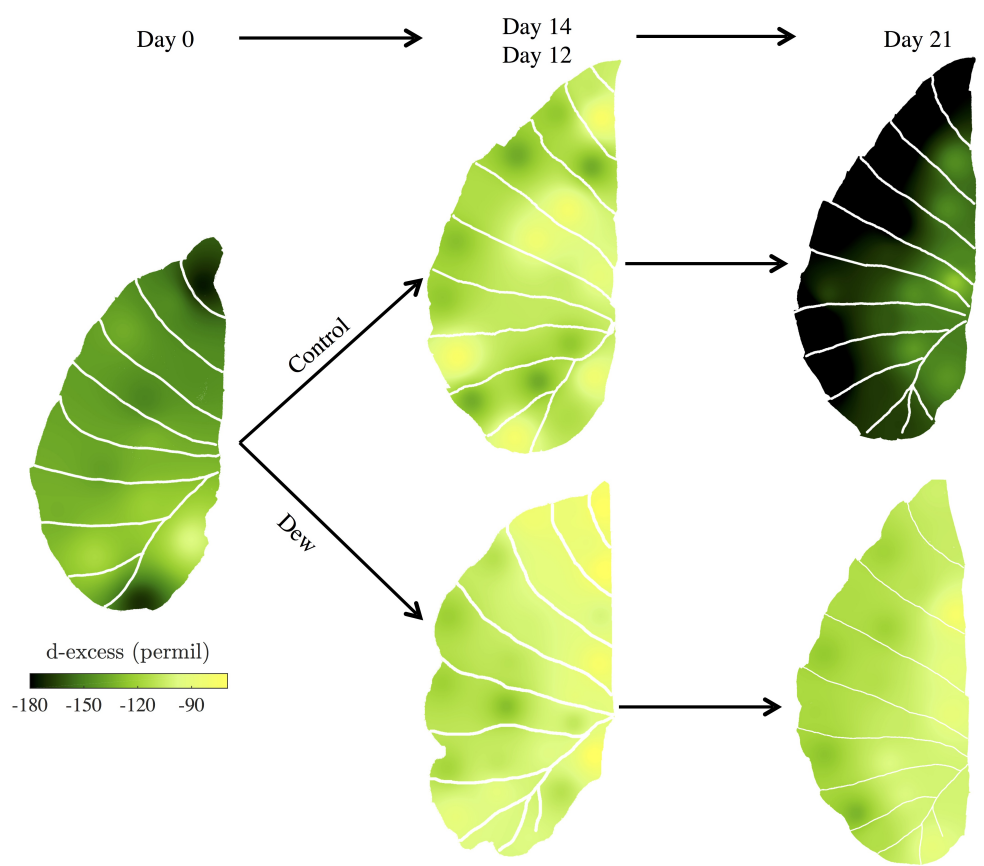


**Figure 2**

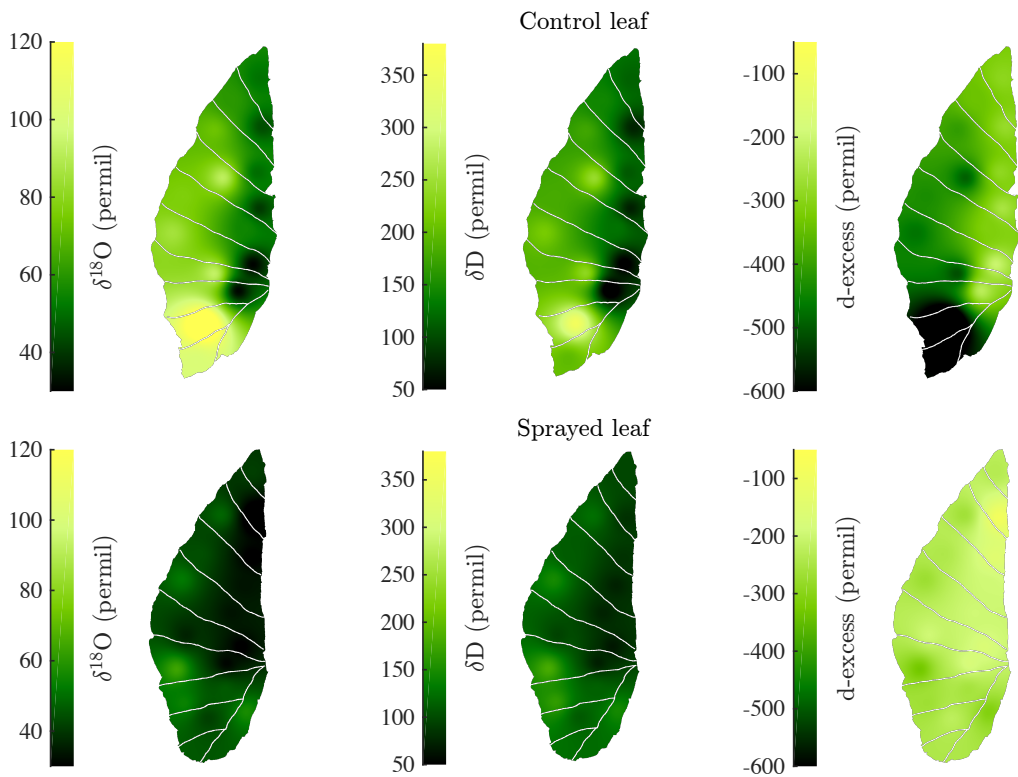


**Figure 3**

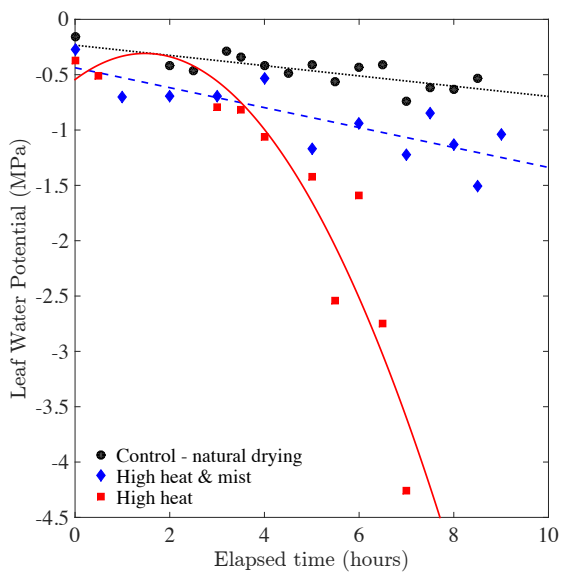


**Figure 4**

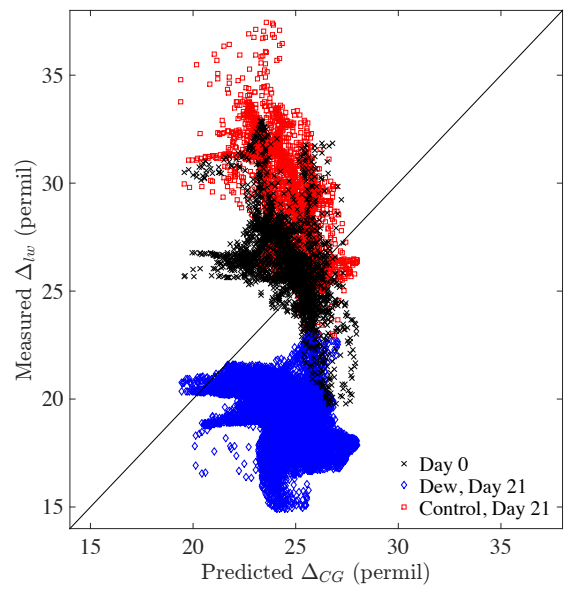


**Figure 5**

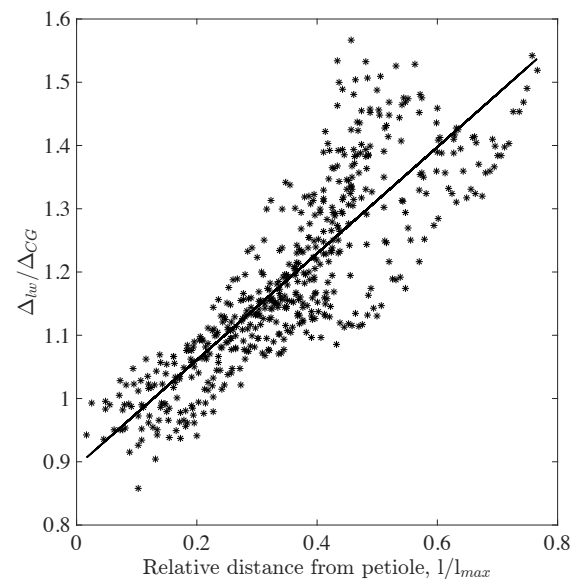


**Figure 6**

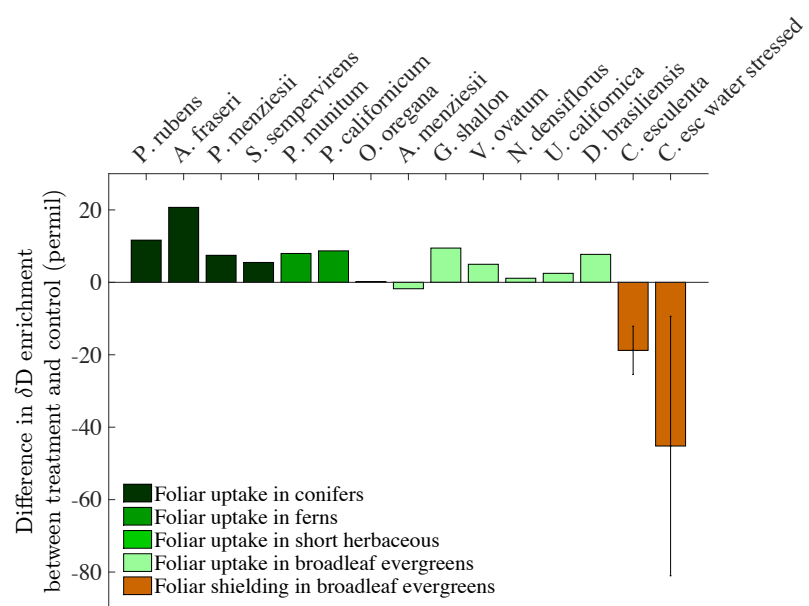


**Figure 7**

## Supplemental Information

**Article title:** The impacts of dew-induced foliar shielding on the energy, water and isotope balance of leaves

**Authors:** Cynthia Gerlein-Safdi, Craig James Sinkler, Kelly Krispin Caylor

The following Supporting Information is available for this article:

**Fig. S1:** Interpolated maps showing the  $\delta D$  of the leaves analyzed in Experiment 1A.

**Fig. S2:** Interpolated maps showing the  $\delta^{18}O$  of the leaves analyzed in Experiment 1A.

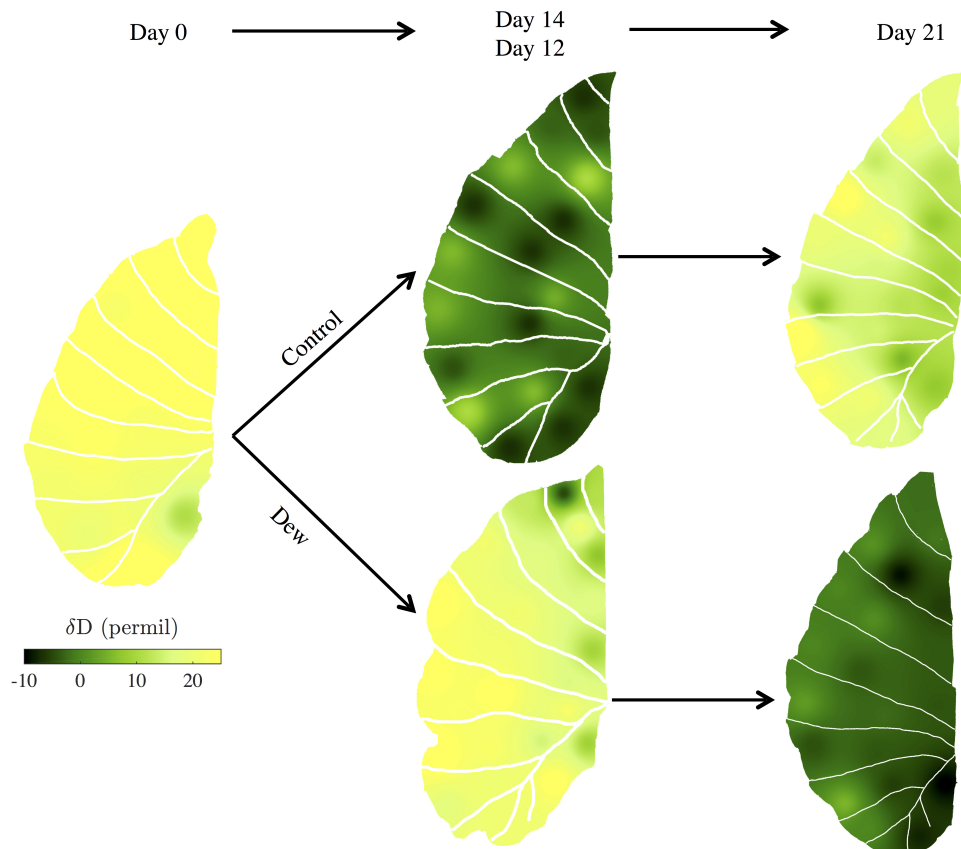


**Figure S1:** Maps of the spacial distribution of  $\delta D$  of five *Colocasia esculenta* leaves collected throughout Experiment 1A. The maps were obtained by inverse distance interpolation of 12 to 25 sampling points analyzed on the Picarro Induction Module. All leaves are c. 38 cm long. **Left:** initial leaf collected on day 0. **Top row:** leaves collected on day 14 (center) and 21 (far right) from the control. **Bottom row:** leaves collected on day 12 (center) and 21 (far right) from the sprayed treatment, where the leaves were sprayed with isotopically enriched water ( $\delta^{18}O \approx 8.85\text{‰}$ ,  $\delta D \approx 737.64\text{‰}$ ) every two days. The color scheme is the same for all rows.

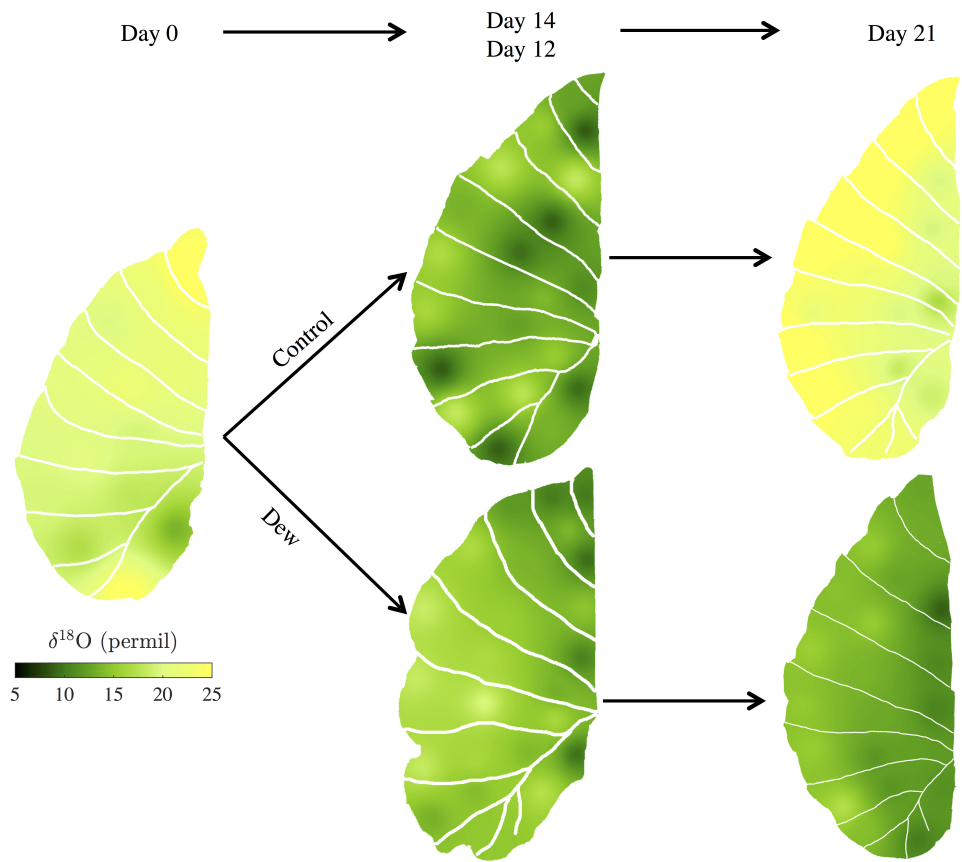


**Figure S2:** Maps of the spacial distribution of  $\delta^{18}\text{O}$  of five *Colocasia esculenta* leaves collected throughout Experiment 1A. The maps were obtained by inverse distance interpolation of 12 to 25 sampling points analyzed on the Picarro Induction Module. All leaves are c. 38 cm long. **Left:** initial leaf collected on day 0. **Top row:** leaves collected on day 14 (center) and 21 (far right) from the control. **Bottom row:** leaves collected on day 12 (center) and 21 (far right) from the sprayed treatment, where the leaves were sprayed with isotopically enriched water ( $\delta^{18}\text{O} \approx 8.85\text{\textperthousand}$ ,  $\delta D \approx 737.64\text{\textperthousand}$ ) every two days. The color scheme is the same for all rows.